European Journal of Cell Biology 102 (2023) 151325

Contents lists available at ScienceDirect

European Journal of Cell Biology

journal homepage: www.elsevier.com/locate/ejcb

Cockayne syndrome group A protein localizes at centrosomes during mitosis and regulates Cyclin B1 ubiquitination

Elena Paccosi [a], Giulia Artemi [a], Silvia Filippi [a], Alessio Balzerano [a], Federico Costanzo [b], Valentina Laghezza-Masci [c], Silvia Proietti [d], Luca Proietti-De-Santis [a,*]

[a] Unit of Molecular Genetics of Aging, Department of Ecology and Biology (DEB), University of Tuscia, 01100 Viterbo, Italy
[b] Faculty of Biomedical Sciences, Institute of Oncology Research, USI, Bellinzona, TI, 6500, Switzerland
[c] Department for Innovation in Biological, Agro-Food and Forest Systems (DIBAF), University of Tuscia, Largo dell'Università, 01100 Viterbo, Italy
[d] Department of Ecological and Biological Sciences, University of Tuscia, 01100 Viterbo, Italy

ARTICLE INFO

Keywords:
Cyclin B1
Centrosome
Mitosis
Cockayne syndrome
Apoptosis
Ubiquitination

ABSTRACT

Mutations in CSA and CSB proteins cause Cockayne syndrome, a rare genetic neurodevelopment disorder. Alongside their demonstrated roles in DNA repair and transcription, these two proteins have recently been discovered to regulate cytokinesis, the final stage of the cell division. This last finding allowed, for the first time, to highlight an extranuclear localization of CS proteins, beyond the one already known at mitochondria. In this study, we demonstrated an additional role for CSA protein being recruited at centrosomes in a strictly determined step of mitosis, which ranges from pro-metaphase until metaphase exit. Centrosomal CSA exerts its function in specifically targeting the pool of centrosomal Cyclin B1 for ubiquitination and proteasomal degradation. Interestingly, a lack of CSA recruitment at centrosomes does not affect Cyclin B1 centrosomal localization but, instead, it causes its lasting centrosomal permanence, thus inducing Caspase 3 activation and apoptosis. The discovery of this unveiled before CSA recruitment at centrosomes opens a new and promising scenario for the understanding of some of the complex and different clinical aspects of Cockayne Syndrome.

1. Introduction

Cockayne syndrome group A (CSA) protein was at first characterized, together with Cockayne syndrome group B (CSB) protein, as playing a role in Transcription Coupled Repair (TCR), the sub-pathway of Nucleotide Excision Repair (NER) specifically aimed to the removal of DNA bulky adducts located on the transcribed strand of active genes (Hanawalt and Spivak, 2008). During TCR, CSA together with CSB protein, first participates in the removal of the RNA polymerase stalled in front of the lesion (Bregman et al., 1996; Svejstrup, 2003) and then in the recruitment of NER proteins, including the transcription/DNA repair factor TFIIH (Lainé and Egly, 2006; van der Weegen et al., 2020).

Mutations in CSA, as well as in CSB, result in Cockayne syndrome (CS) (Henning et al., 1995; Troelstra et al., 1992), a human autosomal recessive disorder characterized by a variety of clinical features, including growth deficiency and severe neurological and developmental manifestations (Karikkineth et al., 2017). However, it has become increasingly clear that some of the features exhibited by CS patients could hardly be attributed to DNA repair deficiencies and that CSA and CSB functions extend far beyond their role in DNA repair. Indeed, the inability of the ultraviolet (UV)-irradiated CS cells to rapidly recover their normal RNA synthesis was shown to be not solely due to the persistence of damage *per se*, since even non damaged genes were switched off (Proietti-De-Santis et al., 2006). Among the years, several other explanations have also been offered including - but not limited to - mitochondrial dysfunction (Okur et al., 2020a; Chatre et al., 2015), prolonged stalling of RNAPII due to defective degradation (Nakazawa et al., 2020) and a failure to degrade transcriptional repressor ATF3 (Epanchintsev et al., 2017; Kristensen et al., 2013).

CSA belongs to the family of WD-40 repeat proteins, known for coordinating interactions among multiprotein complexes (Zhang and Zhang, 2015), and is a component of a ubiquitin E3 ligase complex containing CUL4, RBX1 and DDB1 (Groisman et al., 2003; Fischer et al., 2011). In line with this, it was also found that CSA, as part of the ubiquitin/proteasome machinery together with CSB, was involved in the ubiquitination and further degradation of PRC1 (Mollinari et al., 2002), a microtubule bundling protein involved in the intercellular bridge formation and whose degradation ensure a successful cytokinesis

* Corresponding author.
E-mail address: proietti@unitus.it (L. Proietti-De-Santis).

https://doi.org/10.1016/j.ejcb.2023.151325
Received 30 December 2022; Received in revised form 16 May 2023; Accepted 18 May 2023
Available online 19 May 2023

(Paccosi et al., 2020). Recently, CSA was also shown to have a role in ribosomal biogenesis (Koch et al., 2014; Alupei et al., 2018) and to induce ubiquitination of nucleolin, a nucleolar protein that regulates rRNA synthesis (Okur et al., 2020b).

Cyclin B1 regulates the entry into mitosis and, for this reason, its concentration is finely tuned during cell cycle: it rises in the S phase and peaks during late G2-M phase (Pines and Hunter, 1991; Clute and Pines, 1999). Cyclin B1 is degraded at the metaphase/anaphase transition by a multisubunit complex called APC/C Anaphase Promoting Complex/-Cyclosome (APC/C), which targets cyclin B1 for proteasomal destruction in late mitosis, thus allowing the subsequent mitotic exit (Zachariae, 1999; Harper et al., 2002).

Here, we show how CSA, during promethaphase and metaphase stages, localizes at centrosomes and mediates the ubiquitination of Cyclin B1, lack of this CSA-mediated ubiquitination being associated with caspase 3 activation and apoptosis.

2. Materials and methods

2.1. Cell lines and treatments

MCF-7 cells were grown in DMEM medium supplemented with 10 % Fetal Bovine Serum, 2 mM L-Glutamine and 0,6 ug/mL of insulin from bovine pancreas.

CS3BE is an immortalized CSA line derived from a severely affected individual CS3BE, a compound heterozygote consisting of one CSA allele with a missense mutation (A160V) and a nonsense mutation (E13X)64 (Ridley et al., 2005). CS3BE/CSAwt cells are stably transfected with constructs for conditional expression of the respective WT protein. MRC5 immortalized fibroblast cells in exponential growth phase were transduced with lentiviral shRNA particle (1×10^5 infectious units of virus - Santa Cruz Biotechnology, Santa Cruz, CA, USA), expressing sh-RNA targeting *CSA* or sh-RNA non-targeting control. Puromicin selection (2 μg/mL) is performed to achieve stable gene silencing. Both CS3BE and MRC5 cell lines were grown in DMEM/F10 medium supplemented with 10 % Fetal Bovine Serum and 2mML-Glutamine. Treatment with MG132 50uM was performed for 5 h before extraction procedures.

2.2. Immunofluorescence microscopy

For immunofluorescence experiments, cells were seeded onto Ibidi coverslips. Cells were fixed in ice-cold methanol, washed three times in phosphate buffered saline (PBS), permeabilized in 0.25 %Triton X- 100 in PBS for 10 min, and then blocked in 3 % bovine serum albumin (BSA) in PBS for 30 min before the required primary Abs were applied. The following Abs were employed: anti-Aurora B moAb (AIM-1) (BD Biosciences), rabbit anti-ERCC8 [N2C2] Internal Ab (GeneTex), anti-CSA moAb from IGBMC antibody facility, rabbit anti-γ-tubulin Ab (SIGMA), anti-Cyclin B1 moAb (Santa Cruz biotechnology) and anti-Biotin moAb (Santa Cruz biotechnology). Appropriate secondary Alexa Fluor Ab (ThermoFisher scientific) were used. DNA was marked with DAPI in Vectashield. Slides were analyzed with a confocal microscope system (Zeiss LSM 710) and images were acquired using the interfaced software ZEN 2010. Images were then processed using ImageJ software.

2.3. Cell synchronization

Cells were synchronized with 100 ng/mL nocodazole for 3 h and released to reach the defined mitotic stages.

2.4. Centrosomal isolation and extraction

Centrosomes were isolated as described by Blomber-Wirschell (Blomberg-Wirschell and Doxsey, 1998) and following the improvements of Contadin et al. (2019): briefly, after different times of cell synchronization, mitotic and interphase cell were incubated with 2 μM cytochalasin B and 10 μM nocodazole for 10 min in ice to disrupt MT and actin cytoskeleton. Then, after cells lysis, centrosome were purified and analyzed by Western Blot.

2.5. Western blot

Proteins were fractionated by SDS-PAGE and transferred to nitrocellulose membranes (Bio-Rad) and blotted with respective antibodies.

2.6. Cell cycle analysis

Cells were analyzed with BD Celesta. For cell cycle analysis cells were harvested by trypsinization and fixed with 95 % cold ethanol dropwise until a concentration of 70 % ethanol was reached. Cells were fixed overnight at 4 C followed by centrifugation and resuspension in PBS 1X. For cell cycle analysis cells were incubated for 30 min with 40 μg/mL RNAse A and 15 μg/mL propidium iodide. 30.000 events were counted per condition.

2.7. Plasmid transient transfection

For transient protein expression, plasmid DNA was added to the cells for 48 h using Xtreme gene 9 reagent (Roche).

2.8. Apoptosis assay

A combination of fluorescein diacetate (FDA; 15 μg/mL), propidium iodide (PI, 5 μg/mL), and Hoechst (HO, 2 μg/mL) was used to differentiate apoptotic cells from viable cells. FDA and HO are vital dyes that stain the cytoplasm and nucleus of the viable cells, respectively. The necrotic and the late stage of apoptotic cells are readily identified by PI staining. Approximately 500 randomly chosen cells were microscopically analyzed to determine apoptosis levels.

2.9. Immunoprecipitation assay

CSA-3xFLAG-TY1 protein expression was induced for 24 h by addition of doxycycline to the CS3BE/CSA3xFLAG-TY1 cells. Cells were lysed in RIPA buffer (50 mM Tris-HCl [pH 8], 150 mM NaCl, 1 mM EDTA, 1 % Triton) supplemented with protease-inhibitor mix (Roche), and sonicated before lysate clearance. Centrosomal extracts from cell transfected with pEBB-BT wild- type Ubiquitin (Addgene #36098) vector or with pEBB-BT mutant K48R Ubiquitin and cultured in a medium supplemented with 4uM D-Biotin (SIGMA) were used for pull-down with anti Cyclin B1 antibody coupled to agarose beads by incubating at 4 °C overnight. Beads were then separated from supernatant by centrifugation and thoroughly washed with ice cold PBS before elution procedure. Alternatively, streptavidin magnetic beads (Proteintech) were used for pull-down of biotinylated ubiquitin.

2.10. Statistical analysis

Statistical analysis was performed using the GraphPad software. Where not differently specified, P values were generated using a two-sided t-test to calculate statistical significance.

3. Results

3.1. CSA localizes at centrosomes during prometaphase and metaphase

We recently showed that CSA and CSB proteins, so far strictly considered as nuclear proteins, have a dynamic localization during the cell cycle progression being that at the start of mitosis they relocalize first in the cytoplasm to finally accumulate in the intercellular bridge where they exert their function in Protein Regulator of Cytokinesis 1

(PRC1) ubiquitination and degradation, a step required for a faithful cytokinesis (Paccosi et al., 2020).

Surprisingly, a deeper reading of our results showed that CSA, in addition to its yet described localization, does localize also at the centrosomes during pro-metaphase and metaphase stages. Indeed, CSA, as also schematized in Fig. 1A, is located in the nucleus during interphase (Fig. 1B, panel a), relocalizes to the centrosomes in pro-metaphase and metaphase (Fig. 1B, panel a and Fig. 1C, as evidenced by white arrows), migrates to the cleavage furrow in anaphase (Fig. 1B, panel b) and finally localizes at the intercellular bridge during telophase (Fig. 1B, panel c). In this experiment, Aurora B kinase staining was used to define each mitotic stage, being known its different localizations during mitosis. The use of two different antibodies to stain CSA at the centrosomes in Fig. 1B and Fig. 1C further corroborates the specificity of the signal.

Co-staining with γ-tubulin, one of the major centrosomal components (Khodjakov and Rieder, 1999), in cells at pro-metaphase (Fig. 2A, panel a–c) and metaphase stage (Fig. 2A, panel d-f) further confirmed CSA localization at centrosomes.

We next checked for the localization at centrosomes of Cyclin B1, which is the regulatory subunit of the mammalian M-phase promoting factor (MPF), pivotal for promoting metaphase progression. The co-localization of Cyclin B1 staining with the one of γ-tubulin, as obtained in MCF7 cell line (Fig. 2B, panels a–c), confirmed that Cyclin B1 accumulates at the centrosomes during pro-metaphase and metaphase, stages in which CSA has the same localization.

In order to evaluate if CSA has a role in the control of expression and recruitment of Cyclin B1 at the centrosomes, we analyzed its distribution in patients-derived CSA-deficient (CS3BE) and -rescued (CS3BE + CSA) cells (see M&M). As showed by immunofluorescence studies, lack of CSA expression does not impair the centrosomal recruitment of Cyclin B1, that is in fact correctly positioned at centrosomes in both CS3BE and CS3BE + CSA cells (Fig. 2C, a–c and d-f, respectively). Therefore, our data demonstrated that CSA and Cyclin B1 colocalize at the centrosomes during prometaphase and metaphase (Fig. 2C, panels d-f). As expected, due to the lack of function mutations owned by CS3BE cell line, there is not staining at centrosomes for CSA in these cells (-), thus confirming the antibody specificity (Fig. 2C, panels a–c).

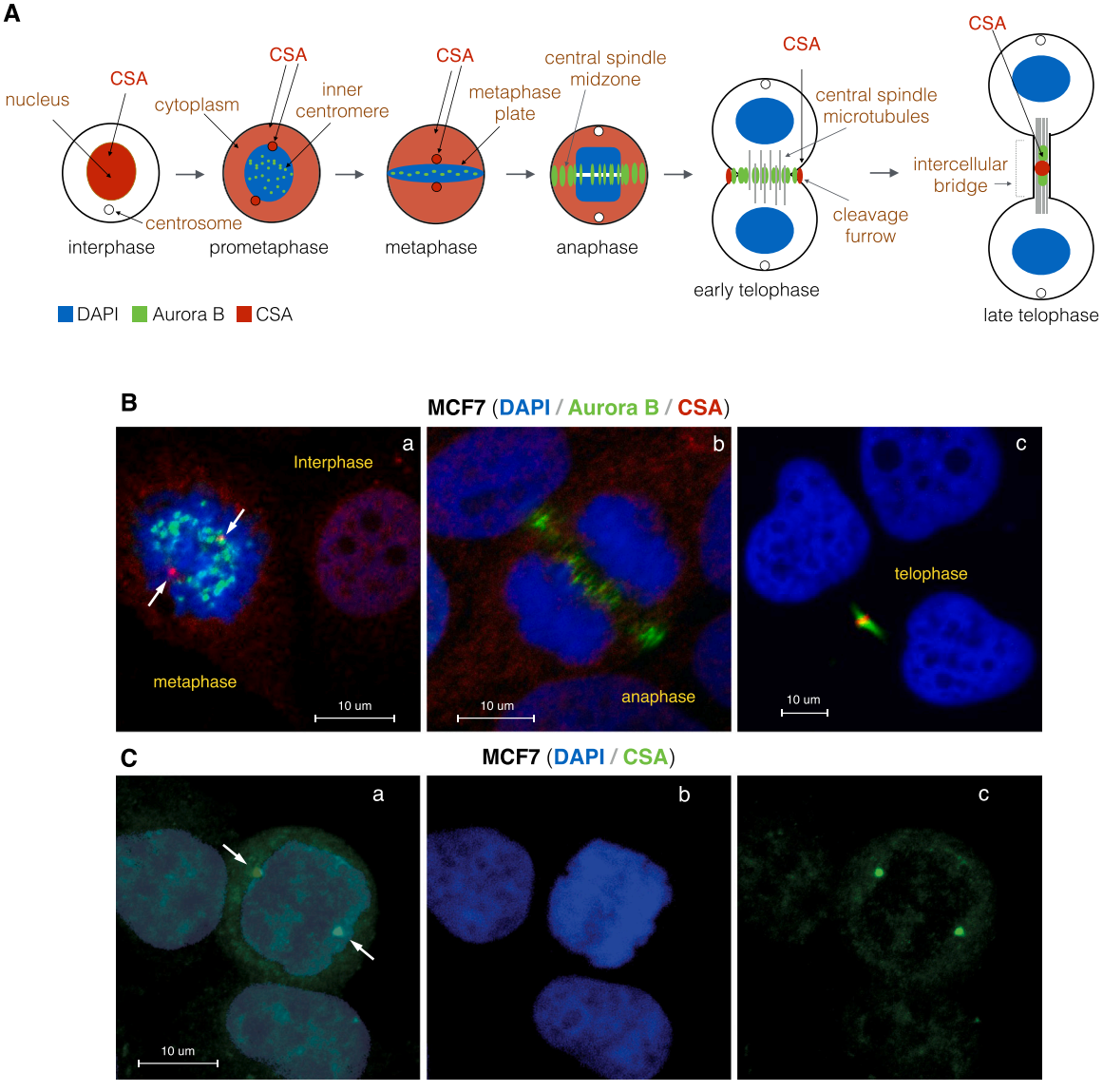

Fig. 1. CSA localizes at centrosomes during prometaphase and metaphase stages. Schematic representation showing the distribution of CSA through the different stages of the cell cycle (**A**). Confocal micrographs of MCF7 cells stained for DNA (blue), Aurora B (green) and endogenous CSA (red) (**B**). Confocal micrographs of MCF7 cells stained for DNA (blue) and CSA (green) (**C**). Each centrosome visualized (n = 50 × 3 exp.) was positive for CSA staining. White arrows indicate centrosomes.

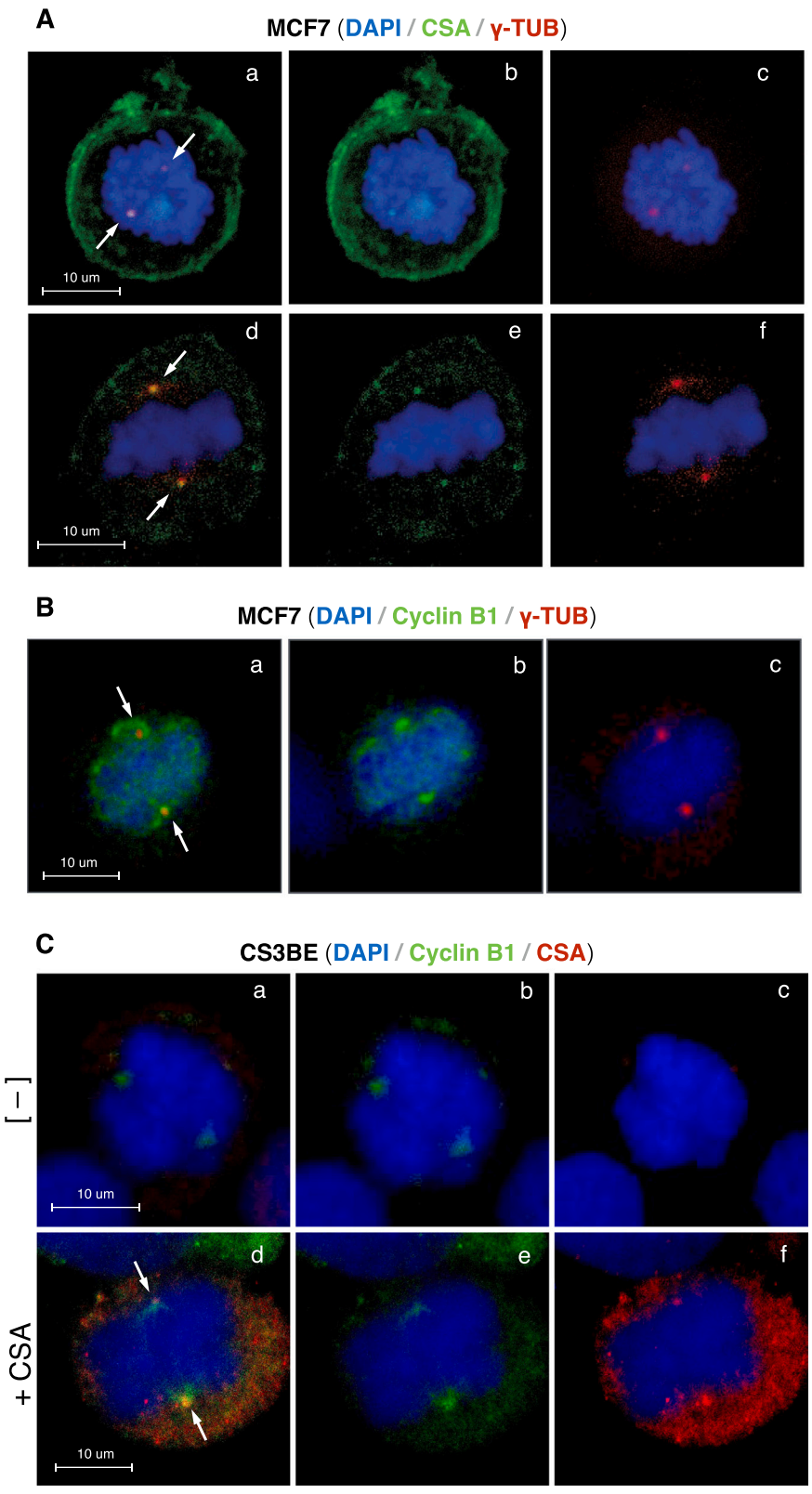

Fig. 2. CSA colocalizes at centrosomes with γ-tubulin and Cyclin B1. Confocal micrographs of MCF7 cells (**A**, **B**) stained for DNA (blue), γ-tubulin (indicated as γ-tub) (red) and endogenous CSA (green) (**A**) or Cyclin B1 (green) (**B**). Each centrosome visualized (n = 50 × 3 exp.) was positive for Cyclin B1 and CSA staining. Confocal micrographs of CS3BE [-] and CS3BE/CSAwt rescued (+CSA) cells stained for DNA (blue), Cyclin B1 (green) and CSA (red) (**C**). Each centrosome visualized (n = 50 × 3 exp.) was positive for Cyclin B1 staining. 72 ± 6 % (n = 50 × 3 exp.) of CS3BE/CSAwt rescued (+CSA) cells was positive for CSA centrosomal staining. White arrows indicate centrosomes.

3.2. CSA regulates the permanence of the Cyclin B1 protein at the centrosome

To biochemically confirm both CSA localization and colocalization with Cyclin B1 at centrosomes, we prepared protein fractions from purified centrosomes from CSA deficient (-) and CSA rescued (+ CSA) metaphase-enriched proliferating cells using the protocol of Blomberg-Wirschell and Doxsey (1998) and following the improvements of Contadini et al. (2019). As schematized in Fig. 3A, different fractions were collected during the procedure: first of all, we recovered the pellet after lysis and centrifugation; next, after Ficoll density gradient centrifugation, we collected both the flow-trough (FT) and the top of the

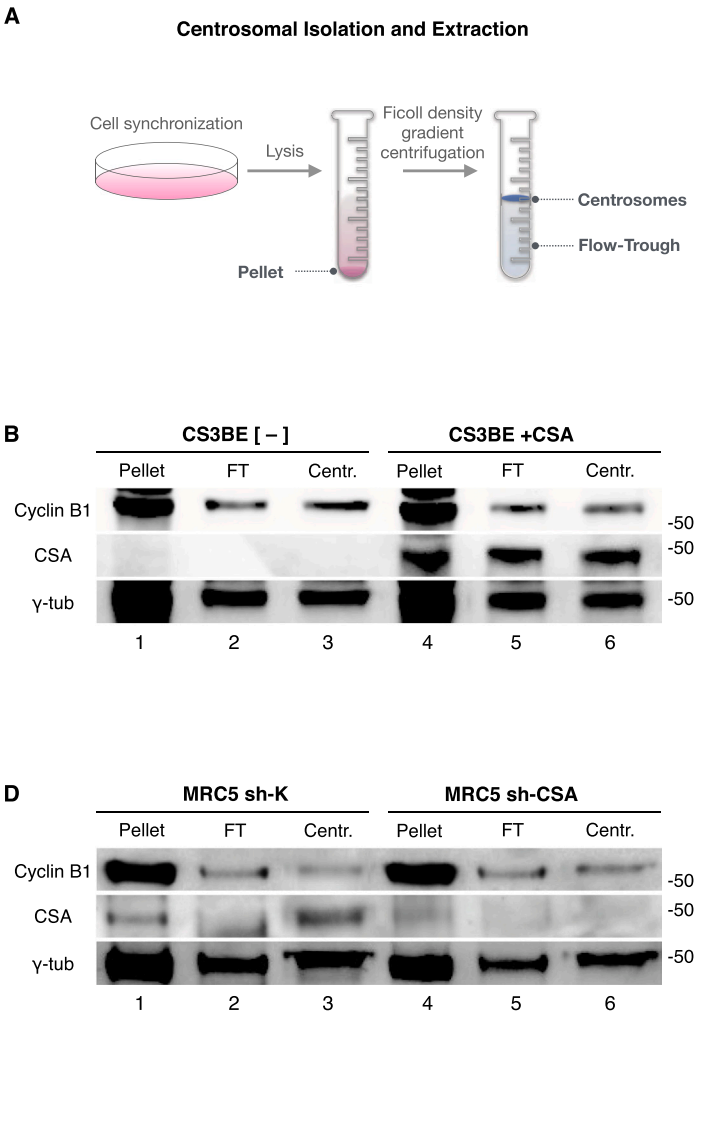

Fig. 3. Cyclin B1 accumulates at centrosomes in cells lacking of CSA. The protocol of Blomber-Wirschell (Clute and Pines, 1999) used to collect the different fractions: at first, after lysis and centrifugation the pellet was recovered; next, after Ficoll density gradient centrifugation, both the flow-trough (FT) and the top of the cushion containing the centrosomal fraction were collected (**A**). Cell fractionation assay showing input, flow-trough (FT) and centrosomal extracts from CS3BE [-] and CS3BE/C-SAwt rescued (+ CSA) cells. Western blot have been performed with antibodies against CSA, γ-tubulin, and Cyclin B1 (**B**). Graphs showing γ-tubulin normalized levels of Cyclin B1 in each fraction (**C**). Cell fractionation assay showing input, flow-trough (FT) and centrosomal extracts from MRC5 sh-K and MRC5 sh-CSA cells. Western blot have been performed with antibodies against CSA, γ-tubulin, and Cyclin B1 (**D**). Graph showing γ-tubulin normalized levels of Cyclin B1 in each fraction (**E**). Data are presented as means (± S.D.) of three independent experiments. *** = $p < 0.001$; ** = $p < 0.01$; n.s. = non significant.

cushion containing the centrosomal fraction. Accordingly with the results obtained by immunofluorescence, in this last fraction we found CSA protein, together with γ-tubulin and Cyclin B1 (Fig. 3B, lane 6). Worthy of note, Cyclin B1 appears to be enriched in centrosomal extracts from CS3BE cells (Fig. 3B, lane 3) as compared to the ones from CSA rescue cell line (Fig. 3B, lane 6). Instead we did not observe any difference in Cyclin B1 levels for what concerns the other fractions. Graph showing the relative Cyclin B1 amount normalized against γ-tubulin, showed that the accumulation of Cyclin B1 observed in CS3BE cells is strictly confined to centrosomes and statistically significative (Fig. 3C).

In order to investigate the behavior of Cyclin B1 in centrosomes, during cell cycle of normal cells which express physiological levels of CSA, we decided to perform the same analysis in MRC5 immortalized fibroblast cells. With this aim we transduced MRC5 cells with lentiviral particles expressing sh-RNA either targeting *CSA* mRNA (sh-CSA) or non-targeting any mRNA as control (sh-K). The effective silencing of CSA was confirmed by Western Blotting (Fig. S1A and relative graph on Fig. S1B). Again, the WB performed on protein fractions from purified centrosomes from MRC5 sh-K and sh-CSA metaphase-enriched proliferating cells, did reveal a significant enrichment of Cyclin B1 in the centrosomal fraction obtained from sh-CSA cells (Fig. 3D compare lane 3 with lane 6), while the other fractions revealed levels of Cyclin B1 similar to the ones obtained from sh-K cells (Fig. 3D compare lanes 1 and 2 with lanes 4 and 5 respectively). These results are resumed in the graph showing Cyclin B1 amount normalized against γ-tubulin (Fig. 3E).

These observations prompted us to assess the centrosomal amount of Cyclin B1 during the metaphase-anaphase transition in presence or not of CSA protein expression. We synchronized both CS3BE and CS3BE+CSA cells in metaphase using nocodazole, since cells treated with this compound can not form metaphase spindles due to deficient polymerization of microtubules. We next "released" the cells from nocodazole, harvesting them at different times from metaphase block, and alternatively purifying centrosomes and total cellular extracts. We then checked for the expression of Cyclin B1 by WB by comparing its content in purified centrosomes and in total cellular extracts. As shown in Fig. 4A, the levels of Cyclin B1, in the centrosomes of CSA rescue cells, undergo a drastic decrease starting from 30 min after the release (Fig. 4A, lanes 7–12), while they remain constant in CS3BE cells (Fig. 4A, lanes 1–6). Worthy of note, the prolonged permanence of Cyclin B1 corresponds to activation of Caspase 3, an unequivocal apoptosis marker, during the next experimental points (Fig. 4A, lanes 4–6). In contrast to what observed in centrosomal fractions, the levels of Cyclin B1 undergo the same physiological decrease in both CS3BE and CS3BE + CSA total cellular extracts (Fig. 4B). Graph showed in Fig. 4C resumes the levels of Cyclin B1 along the entire time course on both total and centrosomal cellular extracts.

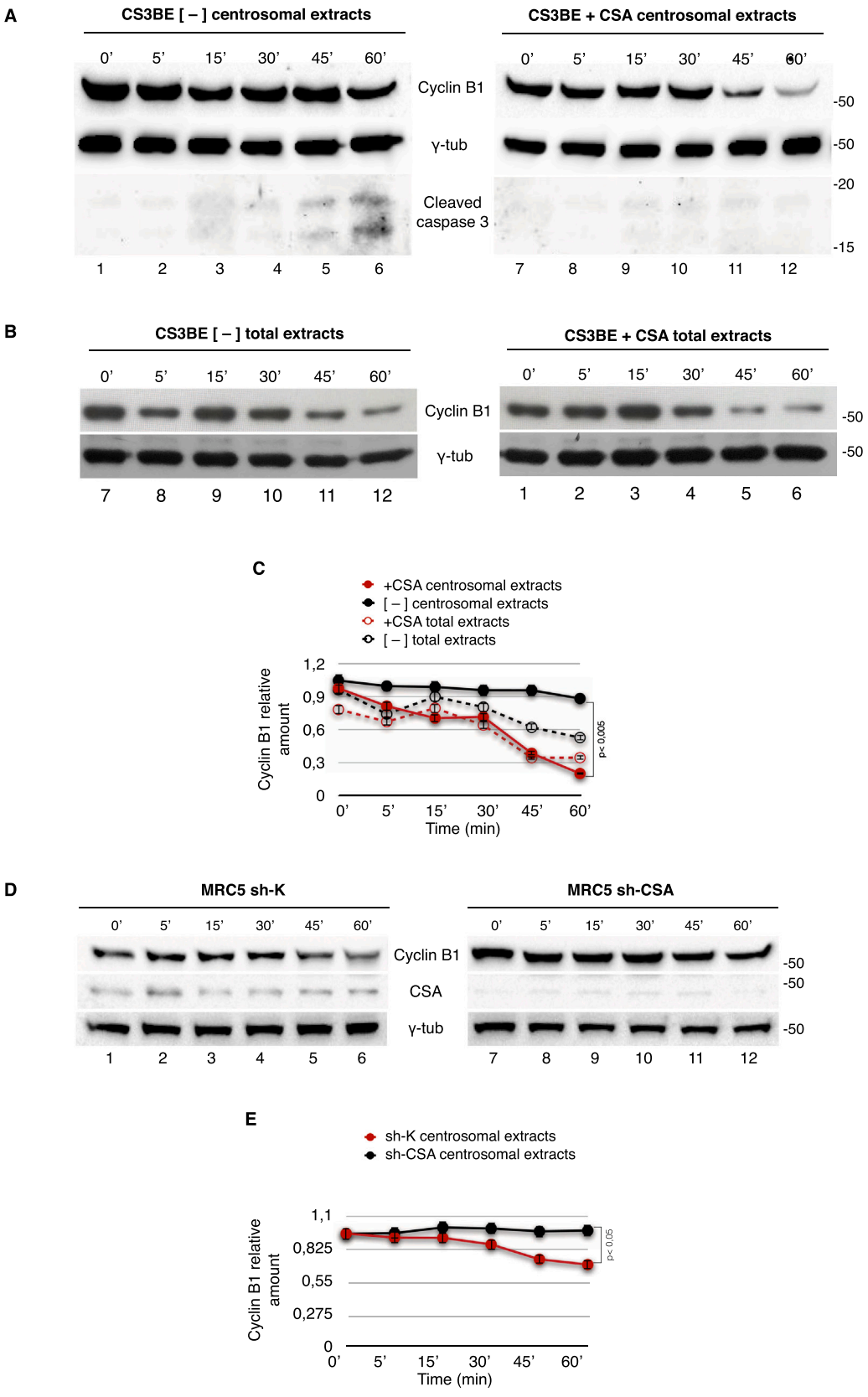

Fig. 4. Cyclin B1 accumulates at centrosomes in cells lacking of CSA, where Caspase 3 is activated. Time course analysis on centrosomal extracts from CS3BE [-] and CS3BE/CSAwt rescued (+ CSA) cells. Western blot has been performed using antibodies against Cyclin B1, γ-tubulin and cleaved caspase 3 (**A**). Time course analysis on total cellular extracts from CS3BE [-] and CS3BE/CSAwt rescued (+ CSA) cells. Western blot has been performed using antibodies against Cyclin B1 and γ-tubulin (**B**). Each Western blot is the representation of three independent biological repeats. Graphs showing relative amount of Cyclin B1 at centrosomes (filled circles) and in total cellular extracts (open circles) (**C**). Time after release from prometaphase block are indicated. Respective line charts represent quantified Cyclin B1 relative amount. Values are from three independent biological repeats (mean ± S.D., one-way ANOVA with Tukey's post hoc test was used for statistical analysis). Time course analysis on centrosomal extracts from MRC5 sh-K and MRC5 sh-CSA cells. Western blot has been performed using antibodies against Cyclin B1, CSA and γ-tubulin (**D**). Each Western blot is the representation of three independent biological repeats. Graphs showing relative amount of Cyclin B1 at centrosomes (**E**). Time after release from prometaphase block are indicated. Respective line charts represent quantified Cyclin B1 relative amount. Values are from three independent biological repeats (mean ± S.D., one-way ANOVA with Tukey's post hoc test was used for statistical analysis).

The same analysis was performed on MRC5 sh-K and sh-CSA cells synchronized in metaphase using nocodazole, released and harvested at the same time points. Again, the levels of Cyclin B1 in purified centrosomes of MRC5 sh-K cells showed a decrease starting from 30 min after the release (Fig. 4D, lanes 4–6), while they remain constant in sh-CSA cells. Graph showed in Fig. 4E resumes the levels of Cyclin B1 along the entire time course on both MRC5 sh-K and sh-CSA centrosomal cellular extracts.

Being aware that the levels of Cyclin B1 are linked to the progression of the cell cycle, we wondered whether the specific lack of degradation of Cyclin B1, as observed in the centrosomes of CS3BE cells, could be due to the eventual arrest of the cells in metaphase. However, cell cycle analysis, performed by flow cytometry, showed that the lack of CSA functionality does not affect metaphase-anaphase transition as well as the entire cell cycle progression (Fig. 5A).

The results of Fig. 4A, showing the activation of the caspase 3, a central component of the apoptotic response network, in metaphase-synchronized CS3BE cells, let us to hypothesize that the apoptosis observed in our experiments, rather than being a phenomenon present in basal conditions, was confined in the time window of metaphase and strictly related to the long-lasting permanence of Cyclin B1 during this stage. Therefore, we decided to deeply investigate this aspect and measure the apoptotic rate displayed by either CS3BE or MRC5 cells, as a function of the CSA functionality. An assay that analyzes the morphological changes that cells display during apoptosis was performed at this scope (Fig. 5B). In order to investigate whether the triggering of the apoptotic process is due to the absence of CSA in the context of its specific role in the Cyclin B1 regulation, we analyzed the rate of apoptosis in the specific phase of the cell cycle in which Cyclin B1 exerts its role, the metaphase-anaphase transition. To this aim, we synchronized the cells in prometaphase and then we analyzed the apoptosis rate at 30 min after release and compared it with that shown by the asynchronously growing cells. In asynchronous cells, lack of CSA expression induces a slight but significant increase of apoptosis (Fig. 5B, panel a for CS3BE and panel d for MRC5 sh-CSA) compared to cells expressing CSA (Fig. 5B, panel b for CS3BE + CSA and panel c for MRC5 sh-K). Instead, metaphase-synchronized cells not expressing or silenced for CSA display a stronger increase in the apoptosis rate (Fig. 5B, panel e for CS3BE and panel h for MRC5 sh-CSA) compared to cells expressing CSA (Fig. 5B, panel f for CS3BE + CSA and panel g for MRC5 sh-K), confirming our hypothesis that CSA ablation/lack of CSA expression makes cells more sensitive to apoptosis during the metaphase of mitosis, displaying the importance of CSA in this specific transition point. Graphs in Figs. 5C and 5D resume the results of this experiment.

3.3. CSA ubiquitinates Cyclin B1

Given the emerging role of CSA in the ubiquitination-degradation process of different target proteins (Okur et al., 2020a; Epanchintsev et al., 2017; Paccosi et al., 2020; Latini et al., 2011; Groisman et al., 2006; Paccosi and Proietti-De-Santis, 2021; Paccosi et al., 2022) we wondered whether Cyclin B1 could be another target of CSA. With this aim, we performed an *in vivo* ubiquitination assay. CS3BE and CS3BE + CSA, MRC5 sh-K and MRC5 sh-CSA cells were transfected with a pEBB-BT-ubiquitin vector for the expression of a *wild-type* ubiquitin tagged with a biotinylation site, and further supplemented with biotin. Alternatively, either CS3BE + CSA or MRC5 sh-K cells were transfected with a mutant K48R pEBB-BT-ubiquitin vector, in which a lysine-to-arginine substitution allows to specifically inhibit the K48-linked polyubiquitination, known to target a protein for degradation by the proteasome, and further supplemented with biotin. In parallel, after 36 h from transfection, a fraction of CS3BE, CS3BE + CSA MRC5 sh-K and MRC5 sh-CSA cells expressing the WT vector were treated with the proteasome inhibitor MG132 for 5 h. Then, all the cells were synchronized with nocodazole and released for 30 min to reach metaphase stage, and centrosomal extraction was performed. First of all, we verified the content of Cyclin B1 in the total centrosomal extracts (input) and we observed, accordingly with our hypothesis, a statistically significant increase of Cyclin B1 in the extracts of CS3BE (Fig. 6A, lane 1 and Fig. S2A) and MRC5 CSA-silenced (Fig. 6B, lane 2 and Fig. S2B) cells, as well as an overall increase of the amount of Cyclin B1 after MG132 treatment (Figs. 6A and 6B, lanes 3 and 4). Next, a Cyclin B1 pull-down from these extracts, followed by blotting against biotin, revealed that the polyubiquitination pattern of Cyclin B1 strongly

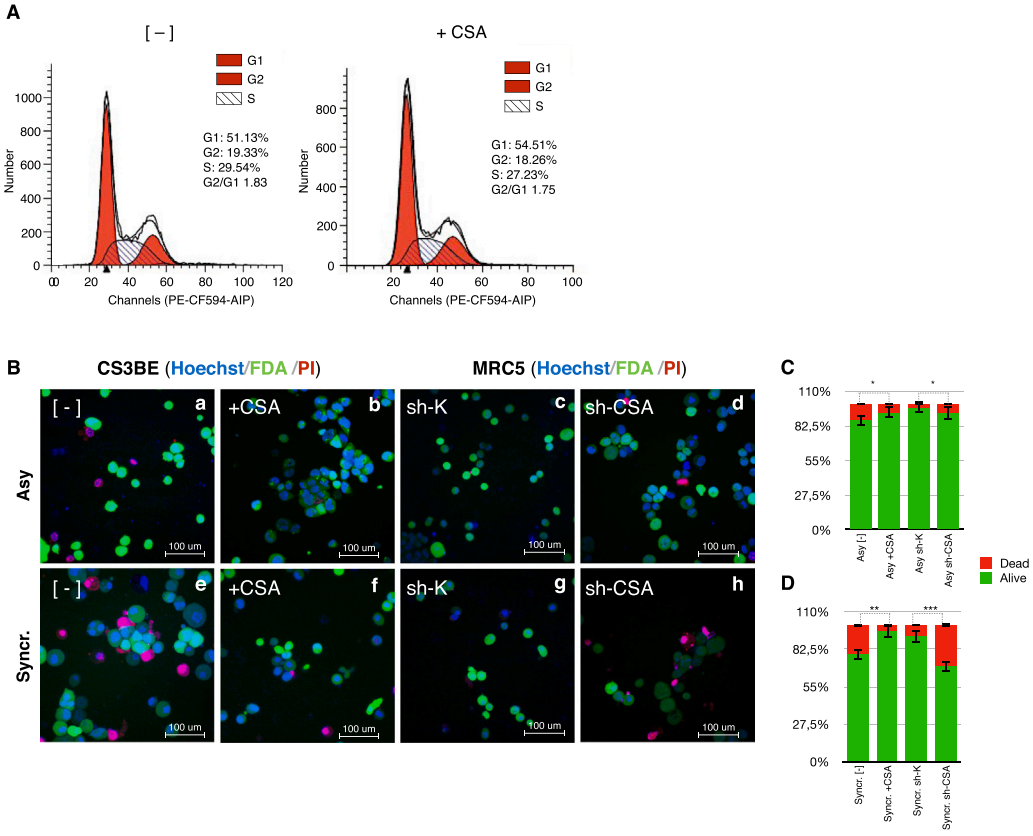

Fig. 5. Cyclin B1 permanence at centrosomes in lack of CSA functionality makes cells more sensitive to apoptosis during the metaphase of mitosis. Cell cycle analysis on CS3BE [-] and CS3BE/CSAwt rescued (+ CSA) cells (**A**). Confocal micrographs of asynchronous and synchronized and released for 30 min CS3BE [-] (panel a and e respectively), CS3BE/CSAwt rescued (+ CSA) (panel b and f respectively), MRC5 sh-K (panel c and g respectively) and MRC5 sh-CSA (panel d and h respectively) cells stained for apoptosis assay with Hoechst (blue), fluorescein diacetate (FDA, green) and propidium iodide (PI, red) (**B**). Graph showing the percentage of alive (green) and dead (red) asynchronous cells from apoptosis assay (n = 500 × 3 independent experiments) (**C**). Graph showing the percentage of alive (green) and dead (red) synchronized cells from apoptosis assay (n = 500 × 3 independent experiments) (**D**). Data are presented as means (± S.D.) of three independent experiments. *** = $p < 0.001$; ** = $p < 0.01$; * = $p < 0.05$.

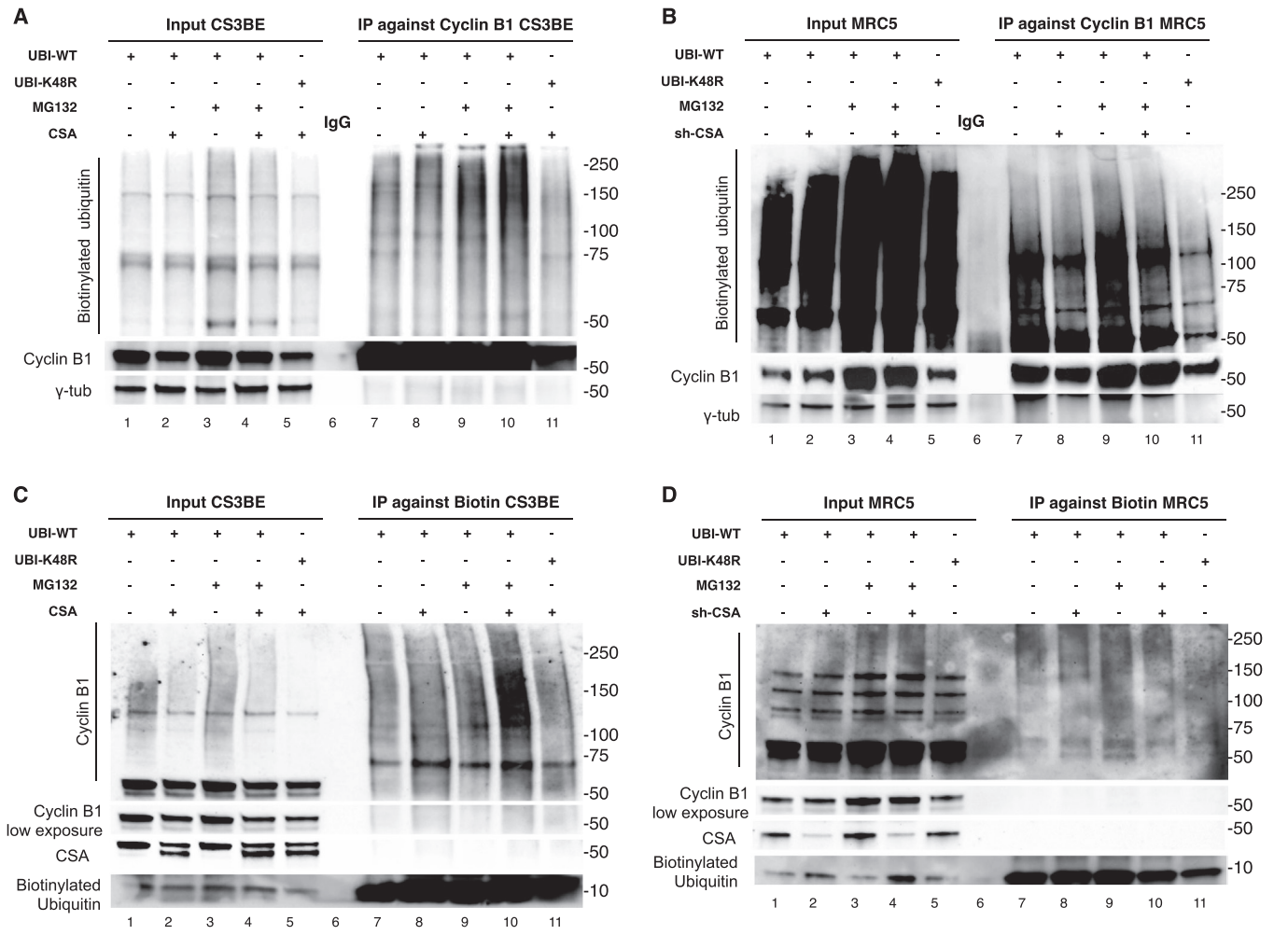

Fig. 6. Centrosomal Cyclin B1 polyubiquitination depends on CSA. Immunoprecipitation of Cyclin B1 from centrosomal extracts of CS3BE [-] and CS3BE/CSAwt rescued (+ CSA) transfected with pEBB-BT-ubiquitin vector and treated or not with MG132 (lanes 7–10) and CS3BE/CSAwt rescued (+ CSA) transfected with pEBB-BT-ubiquitin vector (lane 11). Western blot has been performed using antibodies against Cyclin B1, biotin and γ-tubulin (**A**). Immunoprecipitation of Cyclin B1 from centrosomal extracts of MRC5 sh-K and MRC5 sh-CSA transfected with pEBB-BT-ubiquitin vector and treated or not with MG132 (lanes 7–10) and MRC5 sh-K transfected with pEBB-BT-ubiquitin vector (lane 11). Western blot has been performed using antibodies against Cyclin B1, biotin and γ-tubulin (**B**). Immunoprecipitation of biotinylated ubiquitin from centrosomal extracts of CS3BE [-] and CS3BE/CSAwt rescued (+ CSA) transfected with pEBB-BT-ubiquitin vector and treated or not with MG132 (lanes 7–10) and CS3BE/CSAwt rescued (+ CSA) transfected with pEBB-BT-ubiquitin vector (lane 11). Western blot has been performed using antibodies against Cyclin B1, biotin and CSA (**C**). Immunoprecipitation of biotinylated ubiquitin from centrosomal extracts of MRC5 sh-K and MRC5 sh-CSA transfected with pEBB-BT-ubiquitin vector and treated or not with MG132 (lanes 7–10) and MRC5 sh-K transfected with pEBB-BT-ubiquitin vector (lane 11). Western blot has been performed using antibodies against Cyclin B1, biotin and CSA (**D**). Immunoprecipitation with nonspecific antibody (IgG) has been used as negative control. Input stands for 10 % of the lysate used for the IP. Each Western blot is the representation of three independent biological repeats.

increases when CSA is expressed (Fig. 6A, compare lanes 8 and 7; Fig. 6B, compare lanes 7 and 8), thus suggesting an involvement of CSA in Cyclin B1 regulation by promoting its centrosomal polyubiquitination. Moreover, analyzing the effect of MG132 on the polyubiquitination pattern as a function of CSA expression, we observed a significant increase of the Cyclin B1 polyubiquitination in CSA proficient cells as compared to the CSA deficient ones (Fig. 6A, compare lanes 10 and 9; Fig. 6B, compare lanes 9 and 10). Furthermore, we observed also that the exogenous expression of mutant K48R ubiquitin dramatically impairs the polyubiquitination pattern of Cyclin B1 compared to the WT ubiquitin form (Fig. 6A, compare lanes 11 and 8; Fig. 6B, compare lanes 11 and 7). This experiment confirmed that the Cyclin B1 polyubiquitination pattern is a degradatory specific signal, since it disappeared when the mutant ubiquitin, unable to target the protein for proteasomal degradation, was expressed. Reciprocal experiments, performed by using streptavidin magnetic beads for the pull-down of biotinylated ubiquitin, confirmed the increase in the polyubiquitination pattern of Cyclin B1 as a function of CSA expression (Fig. 6C, compare lanes 8 and 7; Fig. 6D, compare lanes 7 and 8), as well as the significant increase of the Cyclin B1 polyubiquitination pattern in CSA proficient cells after MG132 treatment (Fig. 6C, compare lanes 10 and 9; Fig. 6D, compare lanes 9 and 10). Again, it was confirmed that the exogenous expression of mutant K48R ubiquitin dramatically impairs the polyubiquitination pattern of Cyclin B1 (Fig. 6C, compare lanes 8 and 11; Fig. 6D, compare lanes 7 and 11). Interestingly, the pattern obtained with the mutant form is similar to the one observed in cells lacking CSA expression (Fig. 6C compare lanes 11 and 7; Fig. 6D compare lanes 11 and 8). Furthermore, we analyzed the polyubiquitination pattern displayed by p53, a protein whose ubiquitination has been already described as CSA dependent (Latini et al., 2011) as a control (Fig. S2C).

Altogether, these data demonstrated that CSA is involved in a specific polyubiquitination of Cyclin B1 at the level of the centrosomes, aimed to its degradation.

4. Discussion and conclusions

CSA protein, so far known to be just a nuclear protein, has been recently shown to display a dynamic localization during cell cycle: confined in the nucleus during interphase, it moves away at the start of mitosis to exert its function in the ubiquitination/proteasomal degradation of PRC1 at the level of the midbody, a step required for a faithful cytokinesis (Paccosi et al., 2020). Now, for the first time, we observed the localization of CSA at centrosomes in a strictly determined step of mitosis, starting from pro-metaphase until metaphase exit. Worthy of note, we evidenced a time window in which CSA is positioned at centrosomes together with Cyclin B1, the regulatory subunit of the mammalian M-phase promoting factor (MPF) (Hyver and Le Guyader, 1990). Interestingly, lack of CSA functionality does not affect the Cyclin B1 recruitment at the centrosome but, instead, impairs the ubiquitination of the Cyclin B1 positioned at the centrosome, consequently causing its lasting permanence.

It is well known that Cyclin B1 ubiquitination/degradation is exerted by different E3 ubiquitin ligase complexes to accomplish mitosis: the SCF-type mammalian E3 ligase defined by the F-box containing protein NIPA (SCFNIPA), which times the mitotic entry (Bassermann et al., 2005), and the Anaphase Promoting Complex/Cyclosome (APC/C), which, instead, times the mitotic exit (van Leuken et al., 2008). Apart from the ones described above, during recent years different proteins were found to be involved in Cyclin B1 ubiquitination and degradation, like the ubiquitin-conjugating enzyme Hip2, which seems to be involved in the regulation of Cyclin B1 mediated cell death (Bae et al., 2010), and BRCA1, that regulates Cyclin B1 degradation following DNA damage, contributing to the maintenance of genomic stability (Shabbeer et al., 2013). In this context, we wondered about the role of CSA mediated ubiquitination of the Cyclin B1 positioned at the centrosomes.

Given that, during mitosis, Cyclin B1 localizes in different cellular compartments from centrosomes, to microtubules and chromatin (Bentley et al., 2007), here we show a new and unexpected contribute of the E3 ubiquitin ligase CSA in targeting Cyclin B1 for ubiquitination. Indeed, we demonstrated for the first time the involvement of CSA in Cyclin B1 regulation by promoting its centrosomal polyubiquitination aimed to induce its proteasomal degradation (Fig. 6A–D). However, until now, we were not able to detect CSB protein at the centrosomes, so it is difficult to speculate about a mechanism similar to the one previously observed for PRC1 (Paccosi et al., 2020), where CSA is devoted to its ubiquitination and CSB to the proteasomal degradation step. Further studies will be required to ascertain the absence of CSB involvement in centrosomal Cyclin B1 degradation process since, for all the different target proteins characterized until now, both CS proteins are known to cooperate in the ubiquitination-degradation processes (Okur et al., 2020a; Epanchintsev et al., 2017; Paccosi et al., 2020; Latini et al., 2011; Groisman et al., 2006; Paccosi and Proietti-De-Santis, 2021; Paccosi et al., 2022). It is also possible that, in this case, another protein is responsible for proteasome recruitment to the polyubiquitinated Cyclin B1.

Worthy of note, Cyclin B1 centrosomal permanence in CSA deficient cells is not accompanied by a delay in cell cycle progression. However, the stalling of Cyclin B1 at the centrosome correlates with the activation of Caspase 3, an unequivocal signal of the apoptosis induction. Indeed, centrosomes are well known targets of caspases during apoptosis (Seo and Rhee, 2018) and Cyclin B1 is well known to be a key regulator of apoptosis in various cell types (Gomez et al., 2007). Moreover, it was recently demonstrated that Cyclin B1 overexpression may induces cell death independent of mitotic arrest, even if how Cyclin B1 may drive apoptotic death independent of the cell cycle, to date, is unclear (Eichhorn et al., 2014). Therefore, the failure of CSA deficient cells in ubiquitinating Cyclin B1 may account for a part of the massive apoptosis rate observed in CSA cells (Pascucci et al., 2021).

Moreover, it will be probably of great help to understand if and how the lack of centrosomal CSA might affects cytoskeleton-associated mechanisms that govern either cell division or cell polarity and motility. In highly polarized cells like neurons this phenomenon appears to be particularly detrimental since, in CS models, both stem cell maintenance and differentiation are impaired (Ciaffardini et al., 2014). Given that a polarized organization of the cytoplasm, marked by centrosome localization, has been recently put forward as an early and essential event in the generation of the first neurite and thus neuronal polarization *in vitro* and that centrosome position correlates with the site of first neurite formation (de Anda et al., 2005) it might be possible that CSA, by regulating centrosomal dynamics, could be involved in these processes, thus better explaining some neurological features of CS patients, in addiction to the ones due to transcriptional defects (Sacco, 2013; Wang et al., 2014).

Overall, the involvement of CSA in a cellular function in which CSB seems to not play a part is intriguing and, at the same time, difficult to explain at the level of the phenotype. Indeed, to our knowledge, CSA and CSB are known to play in partnership a plethora of functions ranging from DNA repair to transcription, ribosomal biogenesis, mitochondrial homeostasis and cell cycle regulation (9–17, 19–22). Accordingly, CSA and CSB mutations are known to give rise to the same spectrum of clinical features, suggesting a role in epistatic mechanisms, some of which have been not fully dissected. Further studies will move in the direction of better explaining and dissecting all the implications of CSA recruitment at centrosomes and its possible implication in cell fate and polarization.

CRediT authorship contribution statement

Luca Proietti De Santis: Conceptualization, Writing – original draft. **Elena Paccosi:** Conceptualization, Data curation, Investigation, Formal analysis, Writing – original draft. **Giulia Artemi:** Investigation, Formal analysis. **Silvia Filippi:** Investigation. **Alessio Balzerano**: Investigation. **Federico Costanzo:** Investigation. **Valentina Laghezza-Masci :** Methodology. **Silvia Proietti**: Conceptualization, Formal analysis.

Declaration of Competing Interest

The authors declare that they have no known competing financial interests or personal relationships that could have appeared to influence the work reported in this paper.

Data Availability

Data will be made available on request.

Acknowledgments

Confocal analysis was performed at the Centro Grandi Attrezzature (CGA) of the University of Tuscia. We thank Claudia Contadini and Silvia Soddu (IRCCS Regina Elena National Cancer Institute, Rome, Italy) for fruitful discussions. We also thank Jean-Marc Egly (IGBMC, Strasbourg, France) for providing anti-CSA antibody.

Appendix A. Supporting information

Supplementary data associated with this article can be found in the online version at doi:10.1016/j.ejcb.2023.151325.

References

Alupei, M.C., Maity, P., Esser, P.R., Krikki, I., Tuorto, F., Parlato, R., Penzo, M., Schelling, A., Laugel, V., Montanaro, L., Scharffetter-Kochanek, K., Iben, S., 2018. Loss of proteostasis is a pathomechanism in cockayne syndrome. Cell Rep. 23 (6), 1612–1619. https://doi.org/10.1016/j.celrep.2018.04.041.

Bae, Y., Choi, D., Rhim, H., Kang, S., 2010. Hip2 interacts with cyclin B1 and promotes its degradation through the ubiquitin proteasome pathway. FEBS Lett. 584 (22), 4505–4510. https://doi.org/10.1016/j.febslet.2010.10.016.

Bassermann, F., Peschel, C., Duyster, J., 2005. Mitotic entry: a matter of oscillating destruction. Cell Cycle 4 (11), 1515–1517. https://doi.org/10.4161/cc.4.11.2192.
Bentley, A.M., Normand, G., Hoyt, J., King, R.W., 2007. Distinct sequence elements of cyclin B1 promote localization to chromatin, centrosomes, and kinetochores during mitosis. Mol. Biol. Cell 18 (12), 4847–4858. https://doi.org/10.1091/mbc.e06-06-0539.
Blomberg-Wirschell, M., Doxsey, S.J., 1998. Rapid isolation of centrosomes. Methods Enzym. 298, 228–238. https://doi.org/10.1016/s0076-6879(98)98022-3.
Bregman, D.B., et al., 1996. UV-induced ubiquitination of RNA polymerase II: a novel modification deficient in Cockayne syndrome cells. Proc. Natl. Acad. Sci. USA. 93, 11586–11590. https://doi.org/10.1073/pnas.93.21.11586.
Chatre, L., Biard, D.S., Sarasin, A., Ricchetti, M., 2015. Reversal of mitochondrial defects with CSB-dependent serine protease inhibitors in patient cells of the progeroid Cockayne syndrome. Proc. Natl. Acad. Sci. USA 112 (22), E2910–E2919. https://doi.org/10.1073/pnas.1422264112.
Ciaffardini, F., et al., 2014. The cockayne syndrome B protein is essential for neuronal differentiation and neuritogenesis. Cell Death Dis. 5 (5), e1268 https://doi.org/10.1038/cddis.2014.228.
Clute, P., Pines, J., 1999. Temporal and spatial control of cyclin B1 destruction in metaphase. Nat. Cell Biol. 1 (2), 82–87. https://doi.org/10.1038/10049.
Contadini, C., et al., 2019. p53 mitotic centrosome localization preserves centrosome integrity and works as sensor for the mitotic surveillance pathway. Cell Death Dis. 10 (11), 850. https://doi.org/10.1038/s41419-019-2076-1.
de Anda, F.C., et al., 2005. Centrosome localization determines neuronal polarity. Nature 436, 704–708. https://doi.org/10.1038/nature03811 (PMID: 16079847).
Eichhorn, J.M., Kothari, A., Chambers, T.C., 2014. Cyclin B1 overexpression induces cell death independent of mitotic arrest. PLoS One 9 (11), e113283. https://doi.org/10.1371/journal.pone.0113283.
Epanchintsev, A., et al., 2017. Cockayne's syndrome A and B proteins regulate transcription arrest after genotoxic stress by promoting ATF3 degradation. Mol. Cell 68, 1054–1066. https://doi.org/10.1016/j.molcel.2017.11.009.
Fischer, E.S., et al., 2011. The molecular basis of CRL4DDB2/CSA ubiquitin ligase architecture, targeting, and activation. Cell 147, 1024–1039. https://doi.org/10.1016/j.cell.2011.10.035.
Gomez, L.A., de Las Pozas, A., Reiner, T., Burnstein, K., Perez-Stable, C., 2007. Increased expression of cyclin B1 sensitizes prostate cancer cells to apoptosis induced by chemotherapy. Mol. Cancer Ther. 6 (5), 1534–1543. https://doi.org/10.1158/1535-7163.
Groisman, R., et al., 2003. The ubiquitin ligase activity in the DDB2 and CSA complexes is differentially regulated by the COP9 signalosome in response to DNA damage. Cell 113, 357–367. https://doi.org/10.1016/s0092-8674(03)00316-7.
Groisman, R., et al., 2006. CSA-dependent degradation of CSB by the ubiquitin-proteasome pathway establishes a link between complementation factors of the Cockayne syndrome. Genes Dev. 20 (11), 1429–1434. https://doi.org/10.1101/gad.378206.
Hanawalt, P.C., Spivak, G., 2008. Transcription-coupled DNA repair: two decades of progress and surprises. Nat. Rev. Mol. Cell Biol. 9, 958–970. https://doi.org/10.1038/nrm2549.
Harper, J.W., Burton, J.L., Solomon, M.J., 2002. The anaphase-promoting complex: it's not just for mitosis any more. Genes Dev. 16 (17), 2179–2206. https://doi.org/10.1101/gad.1013102.
Henning, K.A., et al., 1995. The Cockayne syndrome group A gene encodes a WD repeat protein that interacts with CSB protein and a subunit of RNA polymerase II TFIIH. Cell 82, 555–564. https://doi.org/10.1016/0092-8674(95)90028-4.
Hyver, C., Le Guyader, H., 1990. MPF and cyclin: modelling of the cell cycle minimum oscillator. Biosystems 24 (2), 85–90. https://doi.org/10.1016/0303-2647(90)90001-h.
Karikkineth, A.C., et al., 2017. Cockayne syndrome: clinical features, model systems and pathways. Ageing Res. Rev. 33, 3–17. https://doi.org/10.1016/j.arr.2016.08.002.
Khodjakov, A., Rieder, C.L., 1999. The sudden recruitment of gamma-tubulin to the centrosome at the onset of mitosis and its dynamic exchange throughout the cell cycle, do not require microtubules. J. Cell Biol. 146 (3), 585–596. https://doi.org/10.1083/jcb.146.3.585.
Koch, S., Garcia Gonzalez, O., Assfalg, R., Schelling, A., Schäfer, P., Scharffetter-Kochanek, K., Iben, S., 2014. Cockayne syndrome protein A is a transcription factor of RNA polymerase I and stimulates ribosomal biogenesis and growth. Cell Cycle 13 (13), 2029–2037. https://doi.org/10.4161/cc.29018.
Kristensen, U., Epanchintsev, A., Rauschendorf, M.A., Laugel, V., Stevnsner, T., Bohr, V. A., Coin, F., Egly, J.M., 2013. Regulatory interplay of Cockayne syndrome B ATPase and stress-response gene ATF3 following genotoxic stress. Proc. Natl. Acad. Sci. USA 110 (25), E2261–E2270. https://doi.org/10.1073/pnas.1220071110.
Lainé, J.P., Egly, J.M., 2006. When transcription and repair meet: a complex system. Trends Genet. 22, 430–436. https://doi.org/10.1016/j.tig.2006.06.006.
Latini, P., et al., 2011. CSA and CSB proteins interact with p53 and regulate its MDM2-dependent ubiquitination. Cell Cycle 10, 3719–3730. https://doi.org/10.4161/cc.10.21.17905.
Mollinari, C., et al., 2002. PRC1 is a microtubule binding and bundling protein essential to maintain the mitotic spindle midzone. J. Cell Biol. 157, 1175–1186. https://doi.org/10.1083/jcb.200111052.
Nakazawa, Y., et al., 2020. Ubiquitination of DNA damage-stalled RNAPII promotes transcription-coupled repair. Cell 180 (6), 1228–1244. https://doi.org/10.1016/j.cell.2020.02.010.
Okur, M.N., Fang, E.F., Fivenson, E.M., Tiwari, V., Croteau, D.L., Bohr, V.A., 2020a. Cockayne syndrome proteins CSA and CSB maintain mitochondrial homeostasis through NAD+ signaling. Aging Cell. 19 (12), e13268 https://doi.org/10.1111/acel.13268.
Okur, M.N., Lee, J.H., Osmani, W., Kimura, R., Demarest, T.G., Croteau, D.L., Bohr, V.A., 2020b. Cockayne syndrome group A and B proteins function in rRNA transcription through nucleolin regulation. Nucleic Acids Res. 48 (5), 2473–2485. https://doi.org/10.1093/nar/gkz1242.
Paccosi, E., et al., 2020. The Cockayne syndrome group A and B proteins are part of a ubiquitin-proteasome degradation complex regulating cell division. Proc. Natl. Acad. Sci. USA 16, 202006543. https://doi.org/10.1073/pnas.2006543117.
Paccosi, E., Proietti-De-Santis, L., 2021. The emerging role of Cockayne group A and B proteins in ubiquitin/proteasome-directed protein degradation. Mech. Ageing Dev. 195, 111466 https://doi.org/10.1016/j.mad.2021.111466.
Paccosi, E., Balajee, A.S., Proietti-De-Santis, L., 2022. A matter of delicate balance: loss and gain of Cockayne syndrome proteins in premature aging and cancer. Front. Aging 3, 960662. https://doi.org/10.3389/fragi.2022.960662 (PMID: 35935726; PMCID: PMC9351357).
Pascucci, B., Spadaro, F., Pietraforte, D., Nuccio, C., Visentin, S., Giglio, P., Dogliotti, E., D'Errico, M., 2021. DRP1 inhibition rescues mitochondrial integrity and excessive apoptosis in CS-A disease cell models. Int. J. Mol. Sci. 22 (13), 7123. https://doi.org/10.3390/ijms22137123.
Pines, J., Hunter, T., 1991. Human cyclins A and B1 are differentially located in the cell and undergo cell cycle-dependent nuclear transport. J. Cell Biol. 115 (1), 1–17. https://doi.org/10.1083/jcb.115.1.1.
Proietti-De-Santis, L., Drané, P., Egly, J.M., 2006. Cockayne syndrome B protein regulates the transcriptional program after UV irradiation. EMBO J. 25, 1915–1923. https://doi.org/10.1038/sj.emboj.7601071.
Ridley, A.J., Colley, J., Wynford-Thomas, D., Jones, C.J., 2005. Characterisation of novel mutations in Cockayne syndrome type A and xeroderma pigmentosum group C subjects. J. Hum. Genet. 50, 151–154. https://doi.org/10.1007/s10038-004-0228-2.
Sacco, R., 2013. Cockayne syndrome b maintains neural precursor function. DNA Repair 12 (2), 110–120. https://doi.org/10.1016/j.dnarep.2012.11.004.
Seo, M.Y., Rhee, K., 2018. Caspase-mediated cleavage of the centrosomal proteins during apoptosis. Cell Death Dis. 9 (5), 571. https://doi.org/10.1038/s41419-018-0632-8 (PMID: 29752437; PMCID: PMC5948218).
Shabbeer, S., et al., 2013. BRCA1 targets G2/M cell cycle proteins for ubiquitination and proteasomal degradation. Oncogene 32 (42), 5005–5016. https://doi.org/10.1038/onc.2012.522.
Svejstrup, J.Q., 2003. Rescue of arrested RNA polymerase II complexes. J. Cell Sci. 116, 447–451. https://doi.org/10.1242/jcs.00271 (PMID: 12508106).
Troelstra, C., et al., 1992. ERCC6, a member of a subfamily of putative helicases, is involved in Cockayne's syndrome and preferential repair of active genes. Cell 71, 939–953. https://doi.org/10.1016/0092-8674(92)90390.
van der Weegen, Y., et al., 2020. The cooperative action of CSB, CSA, and UVSSA target TFIIH to DNA damage-stalled RNA polymerase II. Nat. Commun. 11, 2104. https://doi.org/10.1038/s41467-020-15903-8.
van Leuken, R., Clijsters, L., Wolthuis, R., 2008. To cell cycle, swing the APC/C. Biochim. Biophys. Acta 1786 (1), 49–59. https://doi.org/10.1016/j.bbcan.2008.05.002.
Wang, Y., et al., 2014. Dysregulation of gene expression as a cause of Cockayne syndrome neurological disease. Proc. Natl. Acad. Sci. USA 111 (40), 14454–14459. https://doi.org/10.1073/pnas.1412569111.
Zachariae, W., 1999. Progression into and out of mitosis. Curr. Opin. Cell Biol. 11 (6), 708–716. https://doi.org/10.1016/s0955-0674(99)00041-1.
Zhang, C., Zhang, F., 2015. The multifunctions of WD40 proteins in genome integrity and cell cycle progression. J. Genom. 3, 40–50. https://doi.org/10.7150/jgen.11015.